

8. A. G. Palmer, C. D. Kroenke, J. P. Loria, *Methods Enzymol.* **339**, 204 (2001).
9. L. K. Nicholson *et al.*, *Nature Struct. Biol.* **2**, 274 (1995).
10. J. C. Williams, A. E. McDermott, *Biochemistry* **34**, 8309 (1995).
11. R. Ishima, D. I. Freedberg, Y. X. Wang, J. M. Louis, D. A. Torchia, *Struct. Fold Des.* **7**, 1047 (1999).
12. L. Wang *et al.*, *Proc. Natl. Acad. Sci. U.S.A.* **98**, 7684 (2001).
13. S. Rozovsky, G. Jogl, L. Tong, A. E. McDermott, *J. Mol. Biol.* **310**, 271 (2001).
14. M. J. Osborne, J. Schnell, S. J. Benkovic, H. J. Dyson, P. E. Wright, *Biochemistry* **40**, 9846 (2001).
15. S. Y. Stevens, S. Sanker, C. Kent, E. R. Zunderweg, *Nature Struct. Biol.* **8**, 947 (2001).
16. S. F. Gothel, M. A. Marahiel, *Cell Mol. Life Sci.* **55**, 423 (1999).
17. P. Rovira, L. Mascarell, P. Truffa-Bachi, *Curr. Med. Chem.* **7**, 673 (2000).
18. S. F. Gothel, M. Herrler, M. A. Marahiel, *Biochemistry* **35**, 3636 (1996).
19. C. Schiene, G. Fischer, *Curr. Opin. Struct. Biol.* **10**, 40 (2000).
20. Y. Zhao, H. Ke, *Biochemistry* **35**, 7362 (1996).
21. \_\_\_\_\_, *Biochemistry* **35**, 7356 (1996).
22. T. R. Gamble *et al.*, *Cell* **87**, 1285 (1996).
23. Y. Zhao, Y. Chen, M. Schutkowski, G. Fischer, H. Ke, *Structure* **5**, 139 (1997).
24. The plasmid containing the gene for human CypA was a generous gift from W. Sundquist. CypA was expressed in BL21/DE3 cells in <sup>15</sup>N-labeled minimal media. Cells were lysed in 25 mM MES, pH 6.1 and 5 mM β-mercaptoethanol and were purified on a S-Sepharose column equilibrated with the same buffer. Remaining DNA was removed on a Q-Sepharose column with 50 mM Tris, pH 7.8 and 5 mM β-mercaptoethanol. NMR sample conditions were 0.43 mM CypA in 50 mM sodium phosphate buffer, pH 6.5, 3 mM dithiothreitol (DTT), 10% D<sub>2</sub>O, with peptide concentrations between 0.04 and 2.6 mM. CypA retained full activity during NMR data collection as determined by the coupled chymotrypsin assay (39), performed on samples before and after each series of relaxation experiments.
25. Spectra were collected on Varian INOVA 600 spectrometers (Varian, Palo Alto, CA) at 25 ± 0.1°C. <sup>1</sup>H-<sup>15</sup>N heteronuclear single-quantum correlation (HSQC) spectra were acquired with the use of WATERGATE (40). <sup>15</sup>N *R*<sub>1</sub>, *R*<sub>2</sub>, [<sup>1</sup>H]-<sup>15</sup>N NOE, and *η*<sub>xy</sub> experiments were performed using pulse sequences reported previously (41, 42). For each sample, at least seven *R*<sub>1</sub> delays and eight *R*<sub>2</sub> delays were acquired, ranging from 100 to 1000 ms and from 10 to 150 ms, respectively. At least four relaxation delays were acquired for the *η*<sub>xy</sub> measurement, ranging from 30 to 120 ms. Spectra were acquired with 2048 and 128 complex points in the <sup>1</sup>H and <sup>15</sup>N dimensions, respectively. Processing and analysis of the NMR spectra were performed with the use of Felix (Accelrys, San Diego, CA). Uncertainties in peak heights were estimated from duplicate spectra. Relaxation rates were determined using the program CurveFit (A. G. Palmer).
26. Additional residues show signs of exchange if the CPMG pulse train is substituted for a single refocusing pulse (12).
27. With addition of the peptide, several residues, including residues N102 and A103, exhibit a decrease in *R*<sub>1</sub>, whereas no significant change is observed for the [<sup>1</sup>H]-<sup>15</sup>N NOE (see the supplementary material for the complete *R*<sub>1</sub> and [<sup>1</sup>H]-<sup>15</sup>N NOE data, available on Science Online at [www.sciencemag.org/cgi/content/full/295/5559/1520/DC1](http://www.sciencemag.org/cgi/content/full/295/5559/1520/DC1)). Thus, for these residues, pico- to nanosecond motions are more restricted in the presence of peptide. A reduction in mobility on this time scale has also been observed for residues 101–104 in the presence of the inhibitor cyclosporin A (35).
28. Single-letter abbreviations for the amino acid residues are as follows: A, Ala; C, Cys; D, Asp; E, Glu; F, Phe; G, Gly; H, His; I, Ile; K, Lys; L, Leu; M, Met; N, Asn; P, Pro; Q, Gln; R, Arg; S, Ser; T, Thr; V, Val; W, Trp; and Y, Tyr.
29. Z. Luz, S. Meiboom, *J. Chem. Phys.* **39**, 366 (1963).
30.  $[S_T] = (\sqrt{(K_D^{obs} - [S_T] + [E_T])^2 + 4[S_T]K_D^{obs}} - (K_D^{obs} - [S_T] + [E_T]))/2$ , where  $[S_T]$  and  $[E_T]$  are the total concentrations of substrate and enzyme, respectively.
31. We first evaluated Eq. 2 in the limit  $k_{ex} \gg \tau_{cp}$ , which amounts to fitting  $K_D^{obs}$  and  $\delta\omega^2/k_{off}$ . This yields a good estimate of  $K_D^{obs}$  (accurate to within approximately 10%), but a poorer estimate of  $\delta\omega^2/k_{off}$  (accurate to within approximately 25%). Knowledge of  $K_D^{obs}$  affords calculation of  $\delta\omega$  from the relation  $\omega_{obs} = \rho_{ES}\delta\omega + \omega_E$ , where  $\omega_{obs}$  and  $\omega_E$  are the chemical shifts observed at a given concentration of substrate and in free CypA, respectively. Note that from the estimated  $K_D^{obs}$  of 1.1 mM,  $\rho_{ES}$  is calculated to 0.67 for the highest substrate concentration used. Subsequently,  $k_{off}$  was estimated by fitting the full Eq. 2 while keeping  $\delta\omega$  fixed. This approach circumvents problems that may otherwise arise when optimizing the individual parameters  $k_{off}$  and  $\delta\omega$ , which appear as a ratio in Eq. 2, simultaneously.
32. Line shape analysis was performed on the peptide in the presence of catalytic amounts of CypA at 25°C with the use of the method described (43) to determine the microscopic rate constants of catalysis.
33. The Bloch-McConnell equations (44) describing the transverse relaxation in the full three-state system (Scheme 1) were integrated numerically with the use of Mathematica 4.0 (Wolfram Research, Champaign, IL), and monoexponential decays were fitted to the resulting data sets, yielding transverse relaxation rates for each residue at each concentration of substrate. The three-state system is underdetermined by the present number of experimental data points. However, starting from parameter values determined separately from line shape analysis of the substrate during catalysis and from the two-site fitting, a sensitivity analysis of the parameter space yields ranges of possible values for the rate constants. The chemical shift differences between the three states were adjusted but kept within a reasonable range. The chemical shift differences between the free and bound states are related to the maximum chemical shift change ( $\delta\omega$ ) observed upon substrate addition and were determined separately by:  $\delta\omega = \delta\omega_{ct}/(1 +$
- $K_{eq}) - \delta\omega_{Et}$ .  $K_{eq} = [ES_{cis}]/[ES_{trans}]$  is obtained from line shape analysis.  $\delta\omega_{ct}$  is the chemical shift difference between  $ES_{cis}$  and  $ES_{trans}$ , and  $\delta\omega_{Et}$  is the chemical shift difference between E and  $ES_{trans}$ .
34. L. D. Zydowsky *et al.*, *Protein Sci.* **1**, 1092 (1992).
35. M. Ottiger, O. Zerbe, P. Guntert, K. Wuthrich, *J. Mol. Biol.* **272**, 64 (1997).
36. An initial structural model of CypA in complex with Suc-Ala-Phe-Pro-Phe-4-NA was built from the crystal structure of CypA in complex with the similar peptide Suc-Ala-Ala-Pro-Phe-4-NA in the cis conformation (PDB entry 1RMH) (27). All structures were viewed and built using MOLMOL (45).
37. Chemical shift changes for this substrate upon binding to cyclophilin have previously been calculated by line shape analysis, and these data also support the proposed model for the conformational change (43).
38. D. Kern, unpublished data.
39. G. Fischer, H. Bang, C. Mech, *Biomed. Biochim. Acta* **43**, 1101 (1984).
40. M. Piotto, V. Saudek, V. Sklenar, *J. Biomol. Nucl. Magn. Reson.* **2**, 661 (1992).
41. N. A. Farrow *et al.*, *Biochemistry* **33**, 5984 (1994).
42. N. Tjandra, A. Szabo, A. Bax, *J. Am. Chem. Soc.* **118**, 6986 (1996).
43. D. Kern, G. Kern, G. Scherer, G. Fischer, T. Drakenberg, *Biochemistry* **34**, 13594 (1995).
44. H. M. McConnell, *J. Chem. Phys.* **28**, 430 (1958).
45. R. Koradi, M. Billeter, K. Wuthrich, *J. Mol. Graph.* **14**, 51 (1996).
46. The microscopic rate constants of substrate interconversion were determined separately from line shape analysis of the peptide NMR spectrum using previously established methods (43).
47. We are grateful to C. Miller for assistance with the quantitative analysis. Supported by NIH grant GM62117 (D.K.) and VR grants K-650-19981661 and S-614-989 (M.A.). Instrumentation grants were awarded by the NSF and the Keck foundation to (D.K.) and by the Knut and Alice Wallenberg foundation (M.A.).

12 September 2001; accepted 11 January 2002

## Role of Nucleoporin Induction in Releasing an mRNA Nuclear Export Block

Jost Enninga,<sup>1</sup> David E. Levy,<sup>2</sup> Günter Blobel,<sup>1\*</sup> Beatriz M. A. Fontoura<sup>1,3</sup>

Signal-mediated nuclear import and export proceed through the nuclear pore complex (NPC). Some NPC components, such as the nucleoporins (Nups) Nup98 and Nup96, are also associated with the nuclear interior. Nup98 is a target of the vesicular stomatitis virus (VSV) matrix (M) protein-mediated inhibition of messenger RNA (mRNA) nuclear export. Here, Nup98 and Nup96 were found to be up-regulated by interferon (IFN). M protein-mediated inhibition of mRNA nuclear export was reversed when cells were treated with IFN-γ or transfected with a complementary DNA (cDNA) encoding Nup98 and Nup96. Thus, increased Nup98 and Nup96 expression constitutes an IFN-mediated mechanism that reverses M protein-mediated inhibition of gene expression.

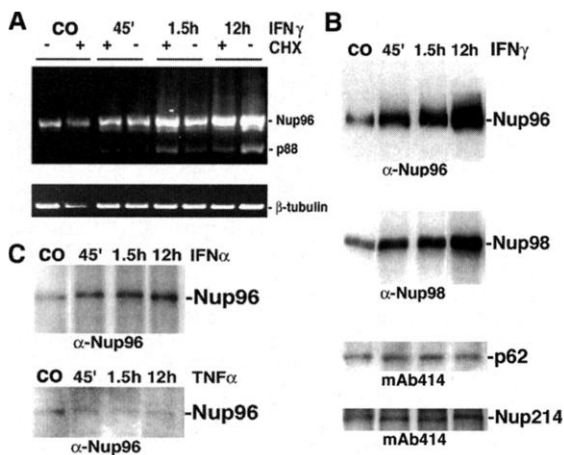
The Nup98 and Nup96 proteins are encoded by a single gene. The primary transcript is alternatively spliced, and the translation products are autocatalytically proteolyzed at one specific site (1–3). Nup98 interacts with an intranuclear protein (4) and transport factors (5, 6). It is involved in nuclear import and export of proteins and RNAs (7–11) and is the target of the VSV M protein-mediated

inhibition of mRNA export (12). A cDNA clone coding for part of the COOH-terminal sequence of Nup96 has been detected among mRNAs that were specifically induced by IFN-γ (13).

We found two classical elements, GAS and ISRE, that mediate increased gene expression by IFN (14, 15). When U937 cells were incubated with IFN-γ for up to 12

REPORTS

**Fig. 1.** Effects of IFN- $\gamma$ , IFN- $\alpha$ , or TNF- $\alpha$  on the expression of some nucleoporins. (A) Levels of various mRNAs (3) at various times after IFN- $\gamma$ -treatment in the presence or absence of cycloheximide (CHX). Controls (CO) were incubated for 12 hours without IFN- $\gamma$ . (B) Immunoblot analysis at various times after IFN- $\gamma$  treatment of U937 cells (3). Equal amounts of protein of total cell lysates were assayed with either mAb414 or with specific antibodies against Nup96 or Nup98 (3). (C) Immunoblot analysis of Nup96 after IFN- $\alpha$  or TNF- $\alpha$  treatment.



hours, we observed an increase in Nup98-Nup96 mRNA levels (Fig. 1A). This induction was not dependent on ongoing protein synthesis, as it was not inhibited by cycloheximide (Fig. 1A). These findings suggest transcription regulation, although other regulatory mechanisms cannot be excluded.

The increased abundance of Nup98-Nup96 mRNA in response to IFN- $\gamma$  was matched by increased amounts of Nup96 and Nup98 proteins. In contrast, there was no significant increase in the amounts of other nucleoporins, such as p62 and Nup214 that react with the monoclonal antibody mAb414 (Fig. 1B; also compare Fig. 3, left panels) (16). As expected, there were increased amounts of the IFN-inducible protein IRF9 (3, 17). Of two other cytokines tested, only IFN- $\alpha$  stimulated Nup96 expression, but to a lesser degree than IFN- $\gamma$ , whereas tumor necrosis factor- $\alpha$  (TNF- $\alpha$ ) had no effect (Fig. 1C).

IFN- $\gamma$  signals through STAT1 homodimers and also regulates the expression of a class of genes in a STAT1-independent manner (14, 18, 19). To determine whether the IFN- $\gamma$ -stimulated expression of Nup98 and Nup96 was mediated by STAT1, we tested STAT1<sup>-/-</sup> or STAT1<sup>+/+</sup> mouse embryo fibroblasts (20) either untreated or treated with IFN- $\gamma$ . An increased expression of Nup98 and Nup96 in response to IFN- $\gamma$  was observed only in the STAT1<sup>+/+</sup> cells but not in STAT1<sup>-/-</sup> cells (Fig. 2), demonstrating the essential role of STAT1 in regulating Nup96 and Nup98 expression.

Immunofluorescence microscopy was

used to test whether the IFN- $\gamma$ -induced Nup98 and Nup96 were properly localized. The IFN- $\gamma$ -stimulated expression of Nup98 (Fig. 3) and of Nup96 yielded an enhanced staining of these proteins at their physiological sites, the NPCs, and the nuclear interior. Thus, both intranuclear and NPC-associated Nup98 and Nup96 may be involved in IFN- $\gamma$ -mediated responses.

VSV replicates in the cytoplasm (21), and VSV M protein inhibits nuclear export of host cell mRNA, ribosomal RNA, and small nuclear RNAs (22) as a mechanism to shut off host cell gene expression. It has been proposed that an interaction of the M protein with Nup98 is the cause of the nuclear export inhibition (12). We tested whether increased expression of Nup98 and Nup96 by IFN- $\gamma$  would reverse this inhibition and restore nuclear export of host cell mRNA. Mouse embryo fibroblasts transfected with a cDNA coding for a green fluorescent protein (GFP)-tagged M protein were incubated in the absence or pres-

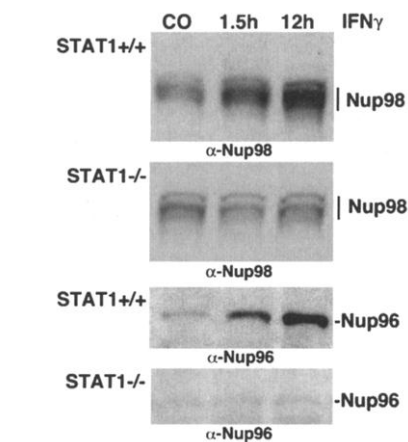


**Fig. 2.** Up-regulation of Nup98 and Nup96 amounts by IFN- $\gamma$  was STAT1-dependent. Shown are immunoblot analysis in STAT1<sup>+/+</sup> or STAT1<sup>-/-</sup> mouse embryo fibroblasts that were incubated for the indicated time periods with IFN- $\gamma$ .

ence of IFN- $\gamma$ . The cellular localization of polyadenylate [poly(A)] containing mRNA was then assessed by in situ hybridization with oligo(dT) (Fig. 4A). In the absence of IFN- $\gamma$ , most of the mRNA was localized in the nucleus of the M protein-transfected cells (upper panel). In contrast, IFN- $\gamma$  treatment of M protein-transfected cells yielded an even distribution of mRNA between the nucleus and the cytoplasm (Fig. 4B). Thus, IFN- $\gamma$  treatment indeed reverses the M protein-mediated inhibition of host cell mRNA export.

IFN- $\gamma$  induces the expression of a wide variety of genes, many of which are involved in antiviral response (23). To determine whether induction of Nup98 and Nup96 was sufficient to reverse the M protein export block, we tested whether transfection with

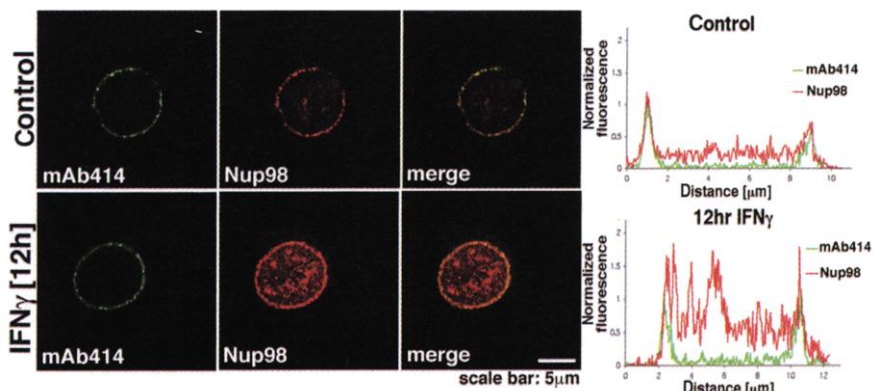


**Fig. 3.** Double immunofluorescence localization of various nucleoporins in U937 cells that were not treated (upper panels) or treated with IFN- $\gamma$  for 12 hours (lower panels). Cells were fixed, permeabilized, and incubated with antibody to Nup98 (red; note staining at nuclear rim and nuclear interior) and mAb414 (green; note primarily nuclear rim staining). The ratio of Nup98 to mAb414 intensities in the equatorial plane of the nucleus was quantified using the Leica TCS spectral confocal microscope software as shown in the graphs at right. Fluorescence intensities were normalized according to the mAb414 intensity that did not significantly change in the absence or presence of IFN- $\gamma$ . Bar, 5 $\mu$ m.

<sup>1</sup>Laboratory of Cell Biology, Howard Hughes Medical Institute, The Rockefeller University, New York, NY 10021, USA. <sup>2</sup>Department of Pathology and Kaplan Comprehensive Cancer Center, New York University School of Medicine, New York, NY 10016, USA. <sup>3</sup>Department of Molecular and Cellular Pharmacology and Sylvester Cancer Center, University of Miami School of Medicine, Miami, FL 33136, USA.

\*To whom correspondence should be addressed. E-mail: blobel@rockvax.rockefeller.edu

## REPORTS

Nup98 and Nup96 cDNA would substitute for IFN- $\gamma$  and relieve the inhibition of mRNA export. Using a luciferase reporter gene assay (24), cells were co-transfected with a mixture of plasmids coding for the M protein alone, for Nup98 and Nup96 alone, or for both. M protein expression clearly inhibited luciferase expression, and this inhibition was partially relieved by Nup98 and Nup96 expression (Fig. 4C). Thus, Nup98 and Nup96 expression is capable of reversing M protein-mediated inhibition of nuclear mRNA export.

The mechanism by which increased expression of Nup98 and of Nup96 reverses M protein-mediated inhibition of mRNA export remains to be elucidated. The inhibitory region of the M protein has been mapped (12, 25) and shown to target the NH<sub>2</sub>-terminal domain of Nup98 (residues 66–515) (12). Nup98 (residues 66–515) contains several distinct domains including

FG (Phe-Gly) repeats that function as docking sites for karyopherins (also termed importins, exportins, or transportins) and a binding site for RanGEF that catalyzes the exchange of guanosine diphosphate for guanosine triphosphate (6, 26). It is conceivable that the M protein interferes with the function of any of these Nup98 domains, resulting in the observed RNA export defects. Overexpression of Nup98 could then compensate for the loss of these functions, thereby reversing the inhibition of RNA export.

Another example for virus interference with nuclear transport at the level of nucleoporins is the polio virus-induced degradation of two specific Nups (Nup153 and p62), which leads to protein import defects (27). Besides playing a key role in antiviral responses, the up-regulation of Nup98 and Nup96 may be involved in other

processes mediated by IFN, such as innate immunity and cell proliferation. Nup98 is a frequent target of chromosomal rearrangements in acute leukemia. Its NH<sub>2</sub>-terminal FG repeat region is present in all leukemia-associated Nup98 fusions that cause chronic and acute myeloid leukemias (28, 29). Nup98 and Nup96 may, thus, play a role in a broad range of activities that can be potentially regulated by different signaling pathways.

### References and Notes

- B. M. A. Fontoura, G. Blobel, M. J. Maturin, *J. Cell Biol.* **144**, 1097 (1999).
- J. S. Rosenblum, G. Blobel, *Proc. Natl. Acad. Sci. U.S.A.* **96**, 11370 (1999).
- Supplementary figure and details of experimental procedures are available on Science Online at [www.sciencemag.org/cgi/content/full/1067861/DC1](http://www.sciencemag.org/cgi/content/full/1067861/DC1).
- B. M. A. Fontoura, S. Dales, G. Blobel, H. Zhong, *Proc. Natl. Acad. Sci. U.S.A.* **98**, 3208 (2001).
- A. Radu, M. S. Moore, G. Blobel, *Cell* **81**, 215 (1995).
- B. M. A. Fontoura, G. Blobel, N. Yaseen, *J. Biol. Chem.* **275**, 31289 (2000).
- X. Wu *et al.*, *Proc. Natl. Acad. Sci. U.S.A.* **98**, 3191 (2001).
- M. A. Powers, D. J. Forbes, J. E. Dahlberg, E. Lund, *J. Cell Biol.* **136**, 241 (1997).
- A. Bachi *et al.*, *RNA* **6**, 136 (2000).
- W. Tan, A. S. Zolotukhin, J. Bear, D. J. Patenaude, B. K. Felber, *RNA* **6**, 1762 (2000).
- W. Hofmann *et al.*, *J. Cell Biol.* **152**, 895 (2001).
- C. von Kobbe *et al.*, *Mol. Cell* **6**, 1243 (2000).
- S.-D. Yang, L. B. Schook, M. S. Rutherford, *Mol. Immunol.* **32**, 733 (1995).
- D. E. Levy, A. Garcia-Sastre, *Cytokine Growth Factor Rev.* **12**, 143 (2001).
- Data on GAS and ISRE elements on Nup98 promoter are not shown.
- L. Davis, G. Blobel, *Cell* **45**, 699 (1986).
- H. A. R. Bluyssen, J. E. Durbin, D. E. Levy, *Cytokine Growth Factor Rev.* **7**, 11 (1996).
- V. Chilakamarti *et al.*, *Proc. Natl. Acad. Sci. U.S.A.* **98**, 6674 (2001).
- M. P. Gil *et al.*, *Proc. Natl. Acad. Sci. U.S.A.* **98**, 6680 (2001).
- J. E. Durbin, R. Hackenmiller, M. C. Simon, D. E. Levy, *Cell* **84**, 443 (1996).
- B. N. Fields, D. M. Knipe, P. M. How, *Fundamental Virology* (Lippincott-Raven Publishers, Philadelphia, ed.3, 1996), pp. 561–575.
- L.-S. Her, E. Lund, J. E. Dahlberg, *Science* **276**, 1845 (1997).
- U. Boehm, T. Klamp, M. Groot, J. C. Howard, *Annu. Rev. Immunol.* **15**, 749 (1997).
- M. Paulson *et al.*, *J. Biol. Chem.* **274**, 25343 (1999).
- J. M. Petersen, L.-S. Her, J. E. Dahlberg, *Proc. Natl. Acad. Sci. U.S.A.* **98**, 8590 (2001).
- M. Dasso, *Cell* **104**, 321 (2001).
- K. E. Gustin, P. Sarnow, *EMBO J.* **20**, 240 (2001).
- H. G. Ahuja, L. Poplewell, L. Tcheurekdjian, M. L. Slovak, *Genes Chromosomes Cancer* **30**, 410 (2001).
- E. Kroon, U. Thorsteinsdottir, N. Mayotte, T. Nakamura, G. Sauvageau, *EMBO J.* **20**, 350 (2001).
- We thank E. J. Smith for assistance with the luciferase assays and E. Izaurralde for generous gifts of VSV M protein plasmids. D.E.L. was supported by AI28900, AI46503, and AI48204 grants from the NIH. B.M.A.F. was also supported by the Florida Biomedical Research Grant (BM025) and by the American Cancer Society Institutional Grant (IRG98-277).

8 November 2001; accepted 8 January 2002

Published online 24 January 2002;

10.1126/science.1067861

Include this information when citing this paper.

**Fig. 4.** IFN- $\gamma$  or Nup98-Nup96 cDNA can reverse the M protein-mediated inhibition of mRNA export. (A) STAT1<sup>+/+</sup> mouse embryo fibroblasts were transfected with a plasmid encoding the GFP-M protein and were incubated in the absence (upper panels) or presence (lower panels) of IFN- $\gamma$ . Oligo(dT) in situ hybridization and fluorescence confocal microscopy was performed as described (3). In the M protein-transfected cell that was not treated with IFN- $\gamma$ , the oligo(dT)-reactive mRNA remained largely in the nucleus, whereas IFN- $\gamma$  treatment of an M protein-transfected cell yielded a nucleocytoplasmic distribution of mRNA resembling that of an adjacent cell which was not transfected by the M protein. (B) STAT1<sup>+/+</sup> or STAT1<sup>-/-</sup> cells were transfected with M protein and incubated in the absence or presence of IFN- $\gamma$ , and the percentage of cells that retained their mRNA in the nucleus was determined. (C) In a luciferase reporter gene expression assay, 293T cells were co-transfected with GFP-M protein, the Nup98-Nup96 cDNAs, or both, as indicated (3).

